Congenital Auditory Deprivation Reduces Synaptic Activity within the Auditory Cortex in a Layer-specific Manner

A. Kral[1,2], R. Hartmann[1], J. Tillein[1], S. Heid[1] and R. Klinke[1]

[1]Physiologisches Institut III, Theodor-Stern-Kai 7, D-60590 Frankfurt am Main, Germany and [2]Institute of Pathological Physiology, Sasinkova 4, SK-811 08 Bratislava, Slovak Republic

The present study investigates the functional deficits of naive auditory cortices in adult congenitally deaf cats. For this purpose, their auditory system was stimulated electrically using cochlear implants. Synaptic currents in cortical layers were revealed using current source density analyses. They were compared with synaptic currents found in electrically stimulated hearing cats. The naive auditory cortex showed significant deficits in synaptic activity in infragranular cortical layers. Furthermore, there was also a deficit of synaptic activities at longer latencies (>30 ms). The 'cortical column' was not activated in the well-defined sequence found in normal hearing cats. These results demonstrate functional deficits as a consequence of congenital auditory deprivation. Similar deficits are likely in congenitally deaf children.

Introduction

Different pathological conditions, e.g. blindness, deafness and amputations, can lead to functional deprivation of the central nervous system. With recent methods it is possible to substitute some of the lost functions (e.g. using cochlear implants). However, patients are often not fully able to exploit the possibilities of such prostheses, as the deprived nervous system has not been sufficiently trained to analyse the afferent activity. Congenital deprivation has the most serious consequences and the resulting deficits may be irreversible. In the visual system, for example, it has been demonstrated that monocular deprivation during a critical period of life (the first 4 months in the cat) influences the functional properties of the primary sensory cortical areas (Hubel and Wiesel, 1970, Blakemore, 1978). The deficits largely persist if initial stimulation takes place after this critical period. Binocular deprivation leads to a substantial reduction in visually responsive cells and loss of their orientation specificity in the primary visual cortex [for a review see e.g. (Rauschecker, 1991)].

Critical periods also appear to exist in the auditory system. Language development, dependent on the auditory system, is known to have a critical period [for a review see (Skuse, 1993)]. Transient expression of acetylcholinesterase, seen in the rat visual and somatosensory cortices during their critical period, is also found in the auditory cortex with a similar time-course (Robertson, 1987; Robertson *et al.*, 1991). The cholinergic system is known to be involved in learning effects in the auditory cortex (Juliano, 1998; Kilgard and Merzenich, 1998; Weinberger, 1998) and might play a role in the formation of thalamocortical connections. Lesion studies, in the cochlea as well as in the central nervous system, support the idea of a critical period in auditory development (Harrison *et al.*, 1991) [for a review of central lesions see e.g. (Wakita and Watanabe, 1997)], as do the data from congenitally deaf individuals equipped with cochlear implants (Eddington *et al.*, 1978; Busby *et al.*, 1992; Fryauf-Bertschy *et al.*, 1997). If congenitally deaf patients are implanted during childhood they can gain complete language competence. However, congenitally deaf patients implanted as adults have significantly poorer auditory performance and do not gain comparable language competence. The deficits in the auditory system responsible for their poor performance remain to be explored.

The congenitally deaf white cat (CDC) is a suitable naturally occurring model of congenital deafness (Larsen and Kirchhoff, 1992; Saada *et al.*, 1996; Heid *et al.*, 1998). CDCs suffer from a dysplasia of the organ of Corti. The inner and outer hair cells are completely missing at an age when hearing starts in normal animals. A similar degeneration (Scheibe dysplasia) is most frequently found in human congenital nonsyndromic sensorineural hearing loss. No further neurological defects have been discovered so far in CDCs (Saada *et al.*, 1996). In contrast to pharmacologically deafened animals (Leake-Jones *et al.*, 1982; Xu *et al.*, 1993; Hardie and Shepherd, 1999), the primary afferents of CDCs are relatively well preserved (90% preservation after 2 years in the basal half turn of the cochlea) (Heid *et al.*, 1998). Only the basal halfturn of the cat cochlea can be reached by cochlear implant electrical stimulation (Hartmann *et al.*, 1997; Kral *et al.*, 1998). Thus the effect of spiral ganglion degeneration does not have to be taken into account in the CDCs, as is the case in pharmacologically deafened animals (Hardie and Shepherd, 1999).

Because of the early degeneration of the cochlea, the auditory cortex of the CDC does not receive any sound-evoked input. Developmental processes dependent on acoustic stimulation cannot take place. However, the brainstem of these animals is anatomically well developed (Heid *et al.*, 1997). The afferent connections of the brainstem show nucleotopic organization (Heid *et al.*, 1997). In their auditory cortex, a rudimentary cochleotopy has been demonstrated by single unit recordings and middle-latency responses (Hartmann *et al.*, 1997).

In the present paper, the question of functional deficits in the acoustically naive auditory cortex is addressed. Indications that abnormalities in neurons, synapses and neuronal connections appear as a consequence of auditory deprivation have been found (Neville and Lawson, 1987; McMullen *et al.*, 1988; Larsen and Kirchhoff, 1992; Chugani *et al.*, 1996; Ponton *et al.*, 1996; Heid *et al.*, 1997; Kotak and Sanes, 1997; Moore *et al.*, 1997; Niparko and Finger, 1997; Hardie *et al.*, 1998; Ryugo *et al.*, 1998; Nishimura *et al.*, 1999; Hardie and Shepherd, 1999; Wurth *et al.*, 1999). Nevertheless, functional data about the deprivation effects on the auditory cortex are not yet available. According to the work of Mitani *et al.* (Mitani *et al.*, 1985) and Prieto *et al.* (Prieto *et al.*, 1994), the different layers of the auditory cortex are activated in a well-defined temporal sequence (Aitkin, 1990). Is this pattern established in congenitally deaf animals? To answer this question, gross synaptic currents in different layers of the auditory cortex were compared between electrically

stimulated normal hearing cats and CDCs using current source density (CSD) analyses.

Materials and Methods

Animals

Two adult normal hearing cats (14 and 21 months of age) and five CDCs (aged between 6 and 29 months) were used. Deafness of the CDCs was verified by the absence of auditory evoked potentials in regular screenings from the age of 4 weeks with intensities up to 125 dB SPL [for details see (Heid *et al.*, 1998)]. Control hearing cats were deafened by an acute intracochlear infusion of neomycin sulphate (1 ml over 5 min) at the beginning of the recordings. The experiments were licensed by the Hessian State Authorities.

Anaesthesia

The animals were preanaesthetized with ketamine (24.5 mg/kg body wt) and xylazine (2.1 mg/kg body wt) i.m. A modified Ringer's solution was applied through a venous catheter (Hartmann *et al.*, 1984, 1997; Kral *et al.*, 1998). Anaesthesia was maintained by additional doses of ketamine. In two CDCs volatile anaesthesia was used after tracheotomy (isoflurane, O_2:N_2O = 1:1). A constant, light level of anaesthesia was ensured by monitoring the EEG, muscle tone, heart rate, end-tidal CO_2, spontaneous movements and withdrawal reflex in response to twitching the forepaw with forceps [details are given in (Kral *et al.*, 1999)].

Surgical Technique and Implant Electrodes

Details of the surgery are given in Hartmann *et al.* (Hartmann *et al.*, 1997). Briefly, the left bulla was exposed and opened, and the round window membrane was carefully removed. A human NUCLEUS 22 electrode (Cochlear Co., Basel) was implanted through the round window (Kral *et al.*, 1998). The NUCLEUS electrode consists of a silastic carrier of <0.65 mm diameter and 22 platinum rings of 0.35 mm width spaced 0.75 mm apart. By convention, the electrode rings are numbered 1–22 from the tip of the electrode. Due to the dimensions of the cat scala tympani, the NUCLEUS implant can only be inserted up to the tenth electrode ring.

Stimulation and Recording

The animals were stimulated with charge-balanced biphasic pulses of 200 μs duration per phase, applied in a bipolar stimulation mode using NUCLEUS electrode rings 2/3.

For recording, the skull was widely opened and the dura above the auditory cortex removed. Recordings were performed with glass microelectrodes filled with Ringer's solution (impedance Z < 6 MΩ) or Elgiloy electrodes (Suzuki and Azuma, 1976) (Z < 6 MΩ). The signal was amplified and band-pass filtered (10 Hz–10 kHz) by a Tektronix 5A22N amplifier, averaged on a Mac II computer (50–100 sweeps dependent on signal/noise ratio, repetition rate 2.1/s). As functional orientation in the auditory cortex in CDCs is not possible, anatomical landmarks were used for orientation. Field potentials were recorded in two parallel rostro-caudal sequences located between the dorsal end of the posterior ectosylvian sulcus (PES) and the anterior ectosylvian sulcus AES (Fig. 1*a*). The distance between the individual recording positions in the rostro-caudal direction was 500 μm, resulting in 14–20 recording positions.

The thresholds of the middle-latency responses were assessed at a position 1 mm rostral and dorsal from the dorsal end of the PES. The field potential thresholds are within a 0–2 dB range from the lowest cortical threshold for apical stimulation electrodes (Popelar *et al.*, 1995; Hartmann *et al.*, 1997) at this standardized position. A stimulus intensity 10 dB above such an evaluated threshold was used for all further recordings. At this high intensity, the amplitude–intensity functions of the middle latency responses are at saturation (Hartmann *et al.*, 1997). The necessary intracochlear current mostly corresponded to 400–500 μApp.

The cortex was penetrated at each recording position (Fig. 1*a*). The electrode was directed perpendicularly to the cortical surface using a stereotactic system. Field potentials were recorded every 150–300 μm to a depth of 3600 μm. Electrode location was controlled by an ORIEL *x*–*y*–*z* positioning device (all three directions controlled with a precision of 1 μm). To avoid tangential tracks, no recordings were made near the sulci. Reproducibility of the recordings was verified by remeasuring the

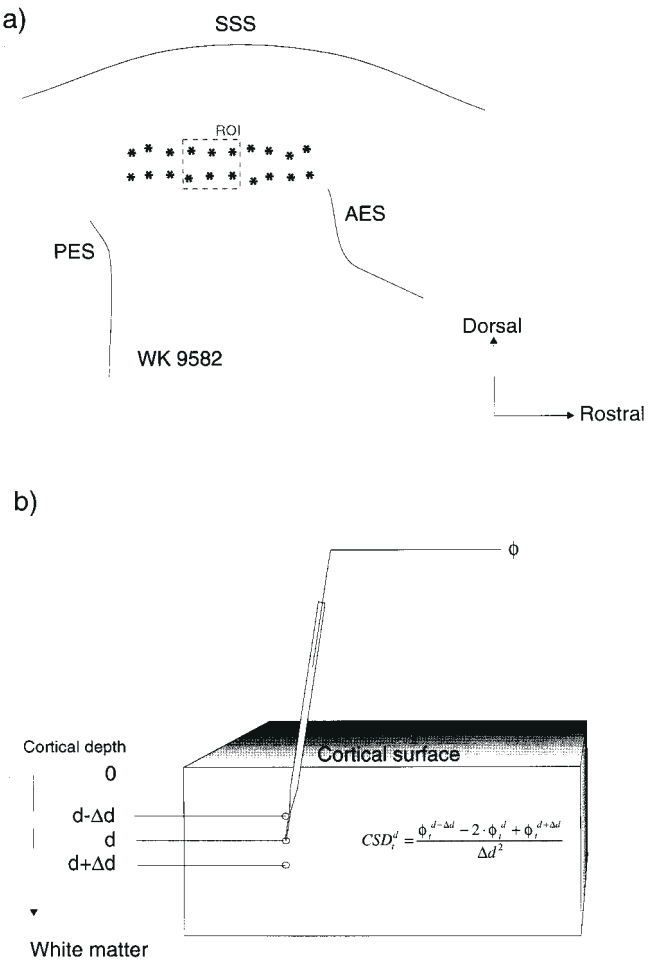

Figure 1. (*a*) Schematic illustration of the track positions in the auditory cortex of animal WK9582. The spacing of the tracks was ~500 μm in both rostro-caudal and ventro-dorsal directions. The rectangle delineates the region of interest (ROI) in this animal. SSS, superior sylvian sulcus; AES, anterior ectosylvian sulcus; PES, posterior ectosylvian sulcus. (*b*) Illustration of the CSD method. Field potentials are recorded with microelectrodes at different depths of the cortex. The one-dimensional CSD equation used to compute the gross synaptic currents is given.

field potentials in several tracks during retraction of the electrode. With Elgiloy electrodes, iron deposits were made to verify both the track angle with respect to the cortical surface and the corresponding recording depths (1000, 2000 and 3000 μm depth, 5–10 μA d.c., 10 s). Sample tracks were marked with iontophoretic application of horseradish peroxidase (2 μA, 10 min) when using glass microelectrodes.

After the experiment, the animals were transcardially perfused [details are given in (Heid *et al.*, 1998)]. The brains were cut on a freezing microtome in 40-μm-thick sections. The sections with iron deposits underwent the Prussian blue reaction (Brown and Tasaki, 1961) and subsequent Nissl staining. In the horseradish peroxidase-marked tracks, the sections were stained with diaminobenzidene (LaVail and LaVail, 1972; Mesulam, 1976), followed by a subsequent Nissl staining. For determination of cortical layers, the angle of the track to the perpendicular direction in respect to cortical surface was defined as the *deviation angle*. Due to a non-zero deviation angle, the depth indicated during the recordings of field potentials by the *x*–*y*–*z* positioning device (*penetration depths*) may not equal the perpendicular distance of the recording positions from the pial surface (*cortical depths*). Therefore, histological track reconstruction was performed in sample tracks, the remaining tracks being reconstructed according to the recording position, the angle of the electrode in the stereotactic device and the stereotactical atlas of the cat brain (Reinoso-Suarez, 1961). The one-

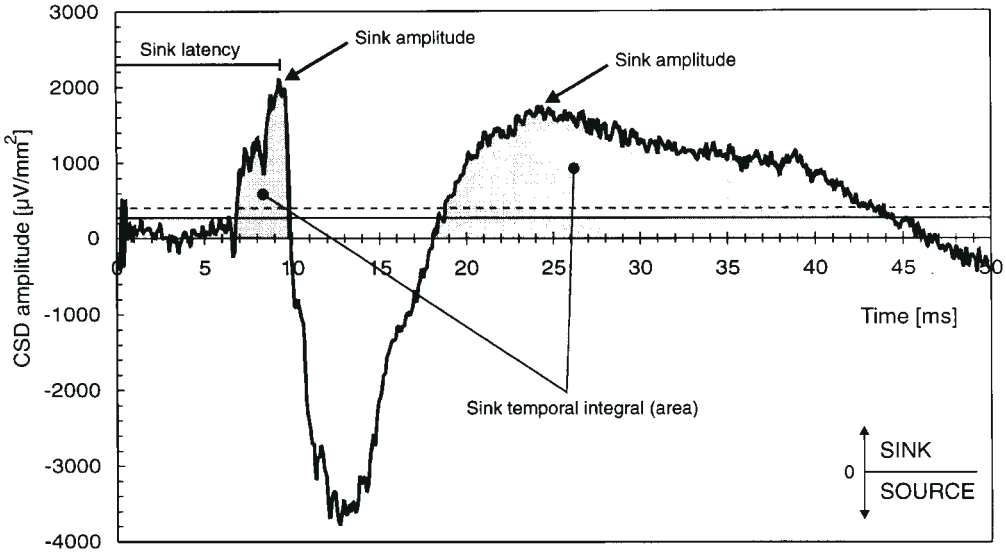

Figure 2. Illustration of the quantitative analysis of the CSD signals. The individual sinks were identified according to the automated procedure, the 'sink temporal integrals' (sink areas) were computed. The maximal amplitudes of each sink were identified ('sink amplitudes') and statistically evaluated. The corresponding latencies ('sink latencies') were also identified. The thresholds for individual sink identification are shown as lines: the solid line represents the maximal noise level of 250 $\mu V/mm^2$, the dashed line the minimal sink amplitude for sink identification (400 $\mu V/mm^2$); for details see text.

dimensional shrinkage of the material (in the track direction) was calculated from the differences in penetration depths *in vivo* and those found in the histological reconstruction. The shrinkage was compensated for.

CSD Analysis

Using extracellular field potentials recorded in different cortical layers, the CSD analysis revealed gross synaptic currents within the investigated tissue at high spatial resolution. Far field effects, e.g. from the thalamus or neighbouring areas of the cortex, are eliminated. The one-dimensional CSD signal represents mainly synaptic currents from vertically oriented cells, predominantly from pyramidal cells (Müller-Preuss and Mitzdorf, 1984).

CSDs (Mitzdorf, 1985) were computed off-line from field potentials (Fig. 1*b*; see Appendix). Each CSD curve was calculated from field potentials at three consecutive depths, resulting in 11 CSD curves in each track. For evaluation of CSD profiles, a region of interest (ROI) was defined (Fig. 1*a*). This was located so that it contained the recording positions with largest P_a waves (first positive wave of the middle latency response). The ROI had dimensions of 1000 μm in the rostro-caudal and 1500 μm in the dorso-ventral direction and comprised 6 tracks in most animals.

An example of computed CSD curves is depicted in Figure 2. The curve shows the CSD over the first 50 ms after the stimulus. Sinks (inward currents with respect to the cellular membrane) are shown as positive deviations of the CSD curve and sources as negative deviations. The sinks of the CSDs correspond to gross synaptic currents, and were shaded in the figures and quantitatively evaluated. In Figure 2, two large sinks can be differentiated, one starting at 7 ms latency and ending at 10 ms latency, the other starting at 18 ms latency and ending at 46 ms latency.

For further evaluation, the sinks were characterised using two measures. Firstly, the maximal amplitudes of each individual sink were determined. These were termed *sink amplitudes* (Fig. 2). The latencies of the sinks were given as peak latencies (i.e. latencies of the sink amplitude) and were termed *sink latencies*. Secondly, the *temporal integrals* ('area' of each sink between its onset and its end) were computed. For these two purposes, the CSD signal was first digitally low-pass filtered using a Hanning window (dimension 2.1 ms), differentiated in time and again filtered by the same Hanning window. To determine a *sink* (maximal amplitude and borders), both the original smoothed curve and the differentiated smoothed curve were used. In an automated evaluation, a sink was accepted when the CSD exceeded at least 250 $\mu V/mm^2$ (which corresponded to peak noise amplitude – solid line in Fig. 2), the sink amplitude was at least 400 $\mu V/mm^2$ (dashed line in Fig. 2) and the sink duration (with amplitude >250 $\mu V/mm^2$) was at least 1.5 ms. The sink amplitudes and the temporal integrals were evaluated from the original CSD curve; the filtered and differentiated curves were used only for the determination of the latencies of the sink onset and maximum amplitude.

To compare the overall synaptic activity in the cortices of individual CDCs to normal cats, CSDs calculated in the ROI were statistically evaluated. For this purpose, the sinks from all layers were pooled. For each animal the mean sink amplitude and the mean temporal integral were computed from the tracks located in the ROI. The normality of sink amplitude and temporal integral distributions were tested with the Pearson–Stephens test (α = 10%). The differences computed were tested for significance with the Wilcoxon–Mann–Whitney test (one-tailed, α = 5%) (Sachs, 1968).

An example of the CSDs is given in Figure 3. The current source densities were computed from three consecutive depths. The CSD signal at 292 μm depth (layer II), for example, was thus computed from the field potentials recorded at 0 (surface), 292 (layer II) and 586 μm (layer III). This CSD signal reflects the gross synaptic currents at 292 μm (layer II). In a simplified view, each CSD sink has corresponding CSD sources at locations above and below, i.e. the large sink at depth 1171 μm is also reflected as a source at 878 μm and the very large source at 1463 μm depth.

Results

Gross Synaptic Currents – Temporal Patterns

The detailed analysis of the gross synaptic currents was performed for the ROI. First, the normal control data were determined. These were then compared with the data from CDCs. Finally, the results were statistically evaluated. Cortical layers were assigned to the penetration depths according to histological reconstruction of dye deposits (for details see Appendix).

Hearing Controls

Figure 3 illustrates a histologically reconstructed track located at the border of the ROI in a normal hearing cat. The cortical field potentials on the left show a positive P_a wave and a negative N_a wave on the surface. The polarity of the first wave reverses at the

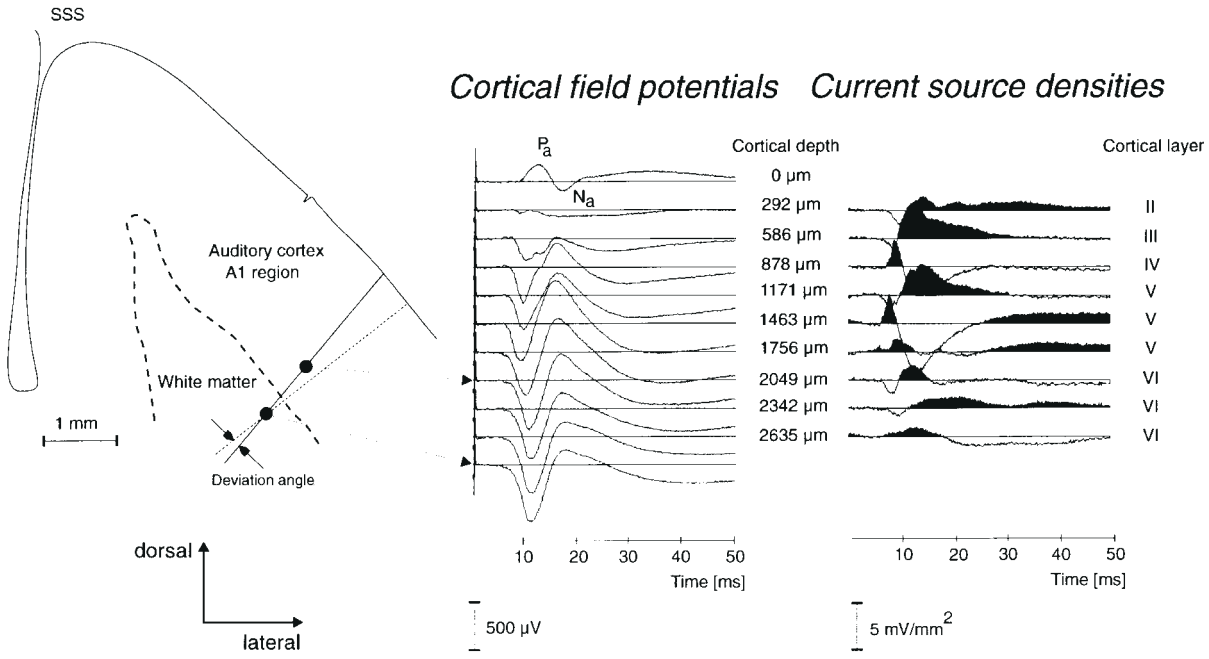

Figure 3. A reconstructed track in the primary auditory cortex of a normal hearing, acutely deafened and electrically stimulated normal animal (cat P110). The brain was sectioned in the frontal direction. The scheme on the left shows two dye deposits (filled circles) in the reconstructed track (solid line). The dashed line crossing the deeper deposit indicates its cortical depth and the deviation angle of the track. Recorded field potentials and corresponding CSD signals are shown. The arrows point to the field potentials recorded at the positions of the dye deposits. In the CSDs the sinks are filled. The layer assignment is on the right. For details see text.

depth of the cortex, so that a prominent negative wave is observed at depths between 586 and 878 µm (layers II and III) and below. A similar polarity reversal was observed with waves corresponding to N_a at the pial surface. There were also differences in the fine structure of the field potentials between different cortical depths.

The activity of the cortical layers had a typical temporal sequence expressed as latency shifts in the current source densities. The sink with the shortest latency is found at depths of 1463 and 1756 µm in Figure 3, which corresponds to infragranular layer V. Subsequently, there is an activation of the cells at 878 µm depth, which is in layer IV. Afterwards, large amplitude and long duration sinks are found at depths of 586 (supragranular, layer III) and 1171 µm (infragranular, layer V). In addition, activation at depths of 2049 and 2635 µm is seen (infragranular, layer VI). Prolonged, low amplitude activation is found at depths of 292 (supragranular, layer II) and 2342 µm (infragranular, layer VI). With onset latencies of over 25 ms, activity is found at depths of 1463 and 1756 µm (infragranular, layer V).

Figure *4a* illustrates a typical field potential track (left) recorded at the position where the P_a wave showed the largest amplitude at the surface (track located inside ROI). The corresponding CSD signals are shown on the right.

A stereotypical temporal sequence of cortical layer activation was found in both normal cats in the ROI:

1. First, infragranular layers V/VI were activated. Next, a small sink was found in layers IV and III. The layer IV sink had a well-expressed fine structure. The short latency sinks, when pooled over the ROI in all layers, showed minimal latencies of 7.2–9 ms; shortest latencies were consistently found for the infragranular layers.
2. Layers III and II were activated afterwards. These sinks had large amplitudes, and their durations reached and exceeded 10 ms. Figure *4a* shows a large sink in both layers III and II (compare also Fig. 3). When pooled over the whole ROI, the sinks in layers II and III showed minimal latencies of 8.4–12.5 ms. In addition, there was a sink of comparable latency in the infragranular layers.
3. Infragranular layers and supragranular layers were then activated in an alternating pattern (latencies >20 ms).

Congenitally Deaf Cats

The CDC with the largest sink amplitudes was selected for comparison in Figure *4b*. The track with the largest P_a amplitude at the surface is shown (located inside ROI). The field potentials and the CSDs differ from those of the hearing cat (Fig. *4a*).

Generally, the CDCs lacked the typical pattern of cortical activation seen in normal cats. The field potentials in the infragranular layers consisted of only small negative waves with ~10 ms latency. In CSDs, there was a substantial reduction of the sink amplitudes with longer latencies. The temporal sequence of synaptic activation of the cortical layers was different in CDCs (Fig. *4b*, right):

1. First, small currents were found in infragranular layers and layer IV (latencies 8.18–9.15 ms). The fine structure of the sinks in the hearing cat, with typical small ripples in the sinks (Fig. *4a*), was missing in CDCs.
2. Next, supragranular layers were activated (10.3–16.7 ms).
3. Longer-latency activations were substantially reduced in naive cortices.

Figure 5 shows the shortest sink latencies found in the ROI in all animals investigated. They are depicted for different penetration depths. The normal cats had almost simultaneous activation at all depths, whereas the CDCs showed greater variation and gen-

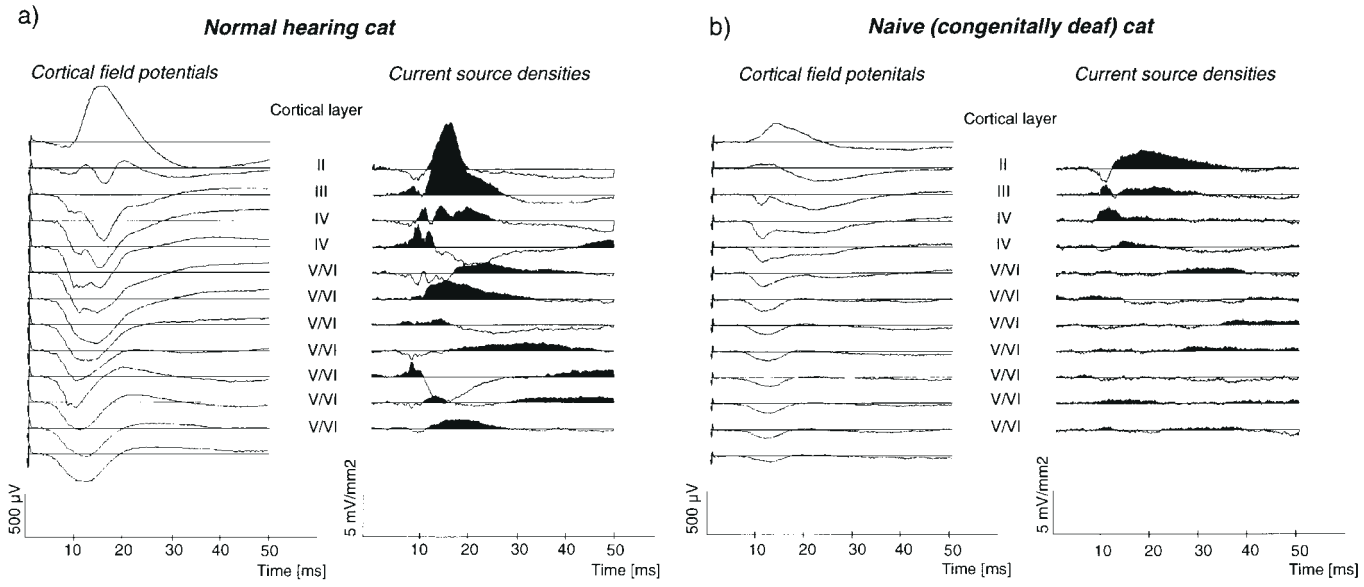

Figure 4. (*a*) Field potentials and CSDs obtained from a normal hearing, acutely deafened and electrically stimulated normal cat (P105). The track is at the position with the maximal P_a wave of the middle-latency response. (*b*) Under the same conditions, signals from a 6-month-old CDC (WK6527). The track is at position with the maximal P_a wave. Low-amplitude field potentials, showing less activity in the deep layers.

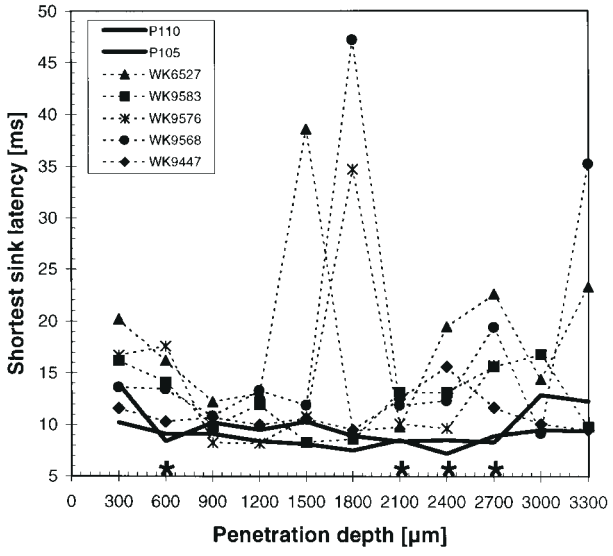

Figure 5. Smallest sink latencies in the corresponding depths from the ROI. Solid lines show the smallest sink latencies from normal cats, dashed lines from CDCs. The CDCs show longer latencies. Statistical significance in corresponding penetration depths is indicated by asterisks. There are large first sink latencies in several CDCs at penetration depths of 1500–1800 µm. Non-significant differences between normal animals and CDCs at depths of 1500–1800 µm are due to large standard deviations in the CDCs (see text).

erally longer latencies. Statistical significance is indicated in the figure by asterisks (two-tailed *t*-test, α = 5%). Significant differences were found for penetration depths of 600 (layer III), 2100, 2400 and 2700 µm (layers V/VI). The shortest sink latencies were also longer in CDCs at depths of 1500–1800 µm (layer V). Because of large standard deviations this difference did not reach statistical significance. As will be shown below, the sinks in infragranular layers with long latencies had small amplitudes.

Table 1
Statistical evaluation of the gross synaptic activity as revealed by the CSDs

Animal	Mean sink integral ($\mu V/mm^2 \cdot ms$)	Mean sink amplitude ($\mu V/mm^2 \cdot ms$)	Max. sink integral	Max. sink amplitude	Age (months)
WK6527	10672.81	1117.08	36618	4033	6
WK9582	10112.66	1026.26	34450.3	4909	18
WK9568	5912.51	578.3	26448	1339	20
WK9576	7917.7	871.78	35471.96	2393	21
WK9447	9593.32	777.9	25766.1	1998	29
Controls					
P105	13404.75	1388.86	61748.6	5380	14
P110	15008.74	1339.85	78499.2	5055	21

P105 and P110 are the control animals, normal hearing, acutely deafened and electrically stimulated by a cochlear implant. For details see text.

Comparison of gross synaptic currents — CSD amplitudes
The mean sink amplitudes, mean temporal integrals of the sinks, maximum values of the sink amplitudes and maximum values of the temporal integrals are shown in Table 1.

Sink Temporal Integrals. In normal cats (P105, P110), the sink integrals (means 13405 and 15009 $\mu V/mm^2 \cdot ms$) were similar, the difference not being significant (Wilcoxon–Mann–Whitney test at α = 5%). Therefore, the data were pooled and compared with the CDCs. The difference in temporal integrals between the controls and the two youngest CDCs (6 and 18 months old) was not significant (mean temporal integrals 10673 and 10112 $\mu V/mm^2 \cdot ms$, Wilcoxon–Mann–Whitney test at α = 5%); the difference between older CDCs and normal cats was significant (mean integrals of 5912–9593 $\mu V/mm^2 \cdot ms$, Wilcoxon–Mann–Whitney test at α = 5%). Of the temporal integrals of the sinks, the largest ones were determined for each animal. These were termed maximum temporal integrals. All CDCs had smaller maximum temporal integrals (~0.5 times smaller).

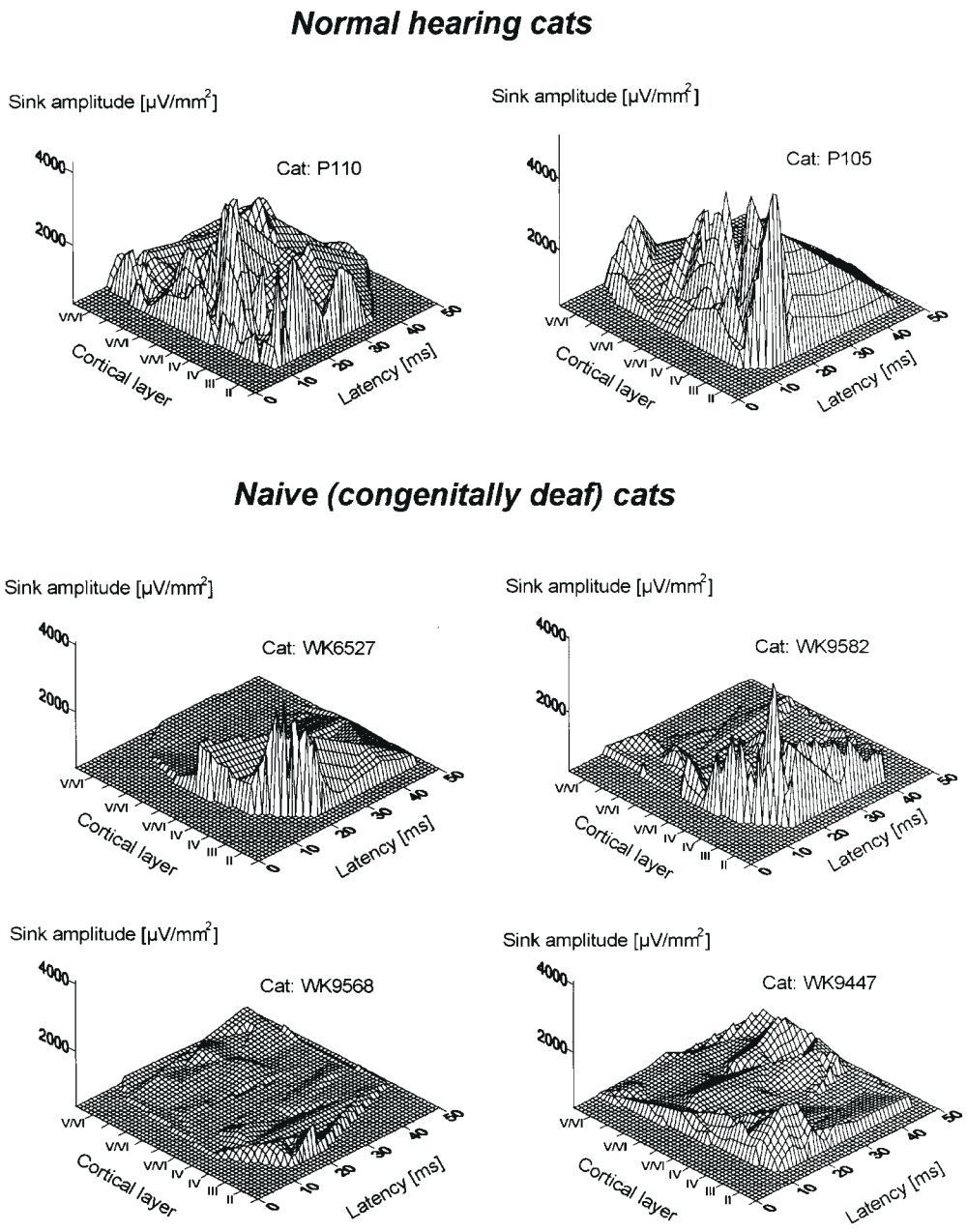

Figure 6. Sink amplitudes pooled from tracks in the ROI (the area at the cortex where largest field potentials were recorded; see Materials and Methods) of individual animals as a function of the corresponding depth and latency. Top: normal hearing, acutely deafened and electrically stimulated normal cats. Almost simultaneous activation of all layers in the ROI is seen when data are pooled. Bottom: the same data from CDCs (animal WK 6527, age 6 months, and WK9582, 18 months; largest mean peaks in the CSDs, largest CSD areas, largest maximal CSD peaks from all CDCs investigated; animal WK9568, age 20 months and WK9447, age 29 months). Successive activation of cortical layers is seen in CDCs with sink latencies of 9–20 ms, shortest onset latencies in infragranular layers. Largest maximal amplitudes are seen in layers II and III.

Sink Amplitudes. The difference in sink amplitudes in the control cats was also not significant (means 1389 and 1340 $\mu V/mm^2$). Again, the data were therefore pooled and compared with those of the CDCs. All CDCs had significantly smaller sink amplitudes (means from 578 to 1117 $\mu V/mm^2$) than normal cats (Wilcoxon–Mann–Whitney test at $\alpha = 5\%$). Of the sink amplitudes, the largest ones were determined for each animal (maximum sink amplitudes). All CDCs had smaller maximum sink amplitudes.

Next, the sink amplitude distribution with respect to cortical layers was investigated. Individual recording tracks represent signals from a topologically restricted column of cortical cells. To minimize the influence of the exact location of individual tracks within the auditory cortex, sink amplitudes were pooled for all tracks within the ROI and presented together for each cat (Fig. 6). This comprised at least six microelectrode tracks in each animal (Fig. 1). For each cortical layer, the sink amplitudes from all six tracks were pooled and depicted at the corresponding latency. Track position information inside the ROI was therefore lost in this presentation. The individual sink amplitudes, as shown in Figure 6 in the layer-latency plane, could have been computed in any of the six tracks in the ROI. Layer specificity, latency and amplitude were preserved.

In normal cats, activation spanned all layers in the latency

range shown (0–50 ms). However, even in the youngest CDCs, the field potentials of which were closest to normal values, the following differences were found: the amplitude of the responses was smaller and not all layers of the cortex were activated as in normal cats. In CDCs the infragranular layers showed only a few small sinks. The supragranular layers were activated with some delay, as also shown in Figure 5. This delay spanned up to 10 ms, with a gradient towards longer latencies at the surface. At longer latencies, the synaptic activity was dramatically reduced, particularly in the infragranular layers.

Influence of Anaesthetics

To rule out the effect of the type of anaesthetic in the activation of the auditory cortex in CDC, two different anaesthetics were used, namely, isoflurane and N_2O in WK6527 and WK9576, and ketamine in all remaining animals. In all animals, the identical criteria of anaesthesia depth were applied (Kral *et al.*, 1999).

The pattern of cortical activation as revealed by CSD analyses did not show any substantial differences. When comparing animals of similar age (e.g. WK6527 to WK9582, and WK9576 to WK9568; see also Fig. 6), the sink amplitudes and sink areas were not significantly different (Wilcoxon–Mann–Whitney, α = 5%).

Discussion

The present study demonstrates the following consequences of congenital auditory deprivation on the auditory cortex:

- significant overall decrease in neuronal excitability by peripheral electrical cochlear stimulation;
- increase in synaptic current latency, particularly in layers III, V and VI; and
- substantial decrease in synaptic activity at longer latencies and in infragranular layers.

These results show substantial deficits in the activity of a naive auditory cortex in response to stimulation of the auditory nerve. Similarly, binocular congenital deprivation leads to a decrease in visually evoked responses of the visual cortical areas, primarily the striate cortex (Yaka *et al.*, 1999). Stryker and Harris showed that a naive visual cortex, following chronic abolition of all afferent neural activity by TTX, lacks the normal segregation of thalamocortical afferents from each eye (Stryker and Harris, 1986). Dark-rearing, which is known to leave spontaneous activity intact, alters the formation of ocular dominance, albeit to a lesser extent (Cynader *et al.*, 1976; Leventhal and Hirsch, 1980; Swindale, 1988). It reduces the percentage of orientation- and direction-selective cells (Imbert and Buisseret, 1975; Buisseret and Imbert, 1976). Dark-rearing also leads to a decrease in the number of dendrites in the visual cortex (Reid and Daw, 1995). Similarly, the number and length of dendrites in the auditory cortex of CDCs are also significantly reduced (Wurth *et al.*, 1999). In the light of this information, congenital deprivation can be expected to lead to a functionally deficient auditory cortex.

Methodological Considerations

The recordings were performed in CDCs at positions that correspond to the field AI in hearing cats. The position in AI was additionally verified by the short latencies of P_a waves [compare (Hartmann *et al.*, 1997)]. The partitioning of auditory cortex and the cytoarchitectonic characteristics of the different compartments are unknown in CDCs. Cell morphology is different in the CDC auditory cortex (Wurth *et al.*, 1999). As a consequence, a reliable identification of AI based on cytoarchitectonics is not possible at present. Further evidence for a recording position in AI is provided by the fact that a rudimentary cochleotopy has been demonstrated in this area of the auditory cortex in CDCs (Hartmann *et al.*, 1997). According to these data, the intracochlear stimulation site used represents the 'best stimulus' for the cortical position evaluated. The stimulating electrodes 2/3 (see Materials and Methods) of the NUCLEUS device lie at a position equivalent to characteristic frequencies of 8–11 kHz in the cochlea (Hartmann *et al.*, 1997). In normal hearing cats, the projection of this cochlear region is located ~2 mm rostral to the posterior ectosylvian sulcus (Merzenich *et al.*, 1975; Reale and Imig, 1980; Phillips and Irvine, 1981). In this study, maximal field potential amplitudes were recorded at approximately this position. There was always a single amplitude maximum with an amplitude decrease in both rostral and dorsal directions. Therefore, the cortical representation of the cochlear portion stimulated is located in the area evaluated (ROI). For the sake of standardization, thresholds of the middle-latency responses were initially determined at a point 1 mm rostral to the dorsal end of the PES. Previous studies have shown that there are no pronounced differences in threshold at this region of AI, although the thresholds increase in the more rostral parts of AI (Hartmann *et al.*, 1997). Final stimulation currents were then fixed at 10 dB above this threshold. With this intensity, a plateau in the electrically evoked amplitude–intensity function of field potentials is safely reached. Thus, a small underestimation of threshold would not cause substantial differences in cortical activation. It should be mentioned that cortical single-units also possess a dynamic range of 10 dB with pulsatile electrical stimulation (Hartmann *et al.*, 1997).

The microelectrode possesses a distance sensitivity of ~30 μm (Sugimoto *et al.*, 1997). Recording steps of 300 μm during microelectrode tracks correspond to previous studies in the auditory cortex (Müller-Preuss and Mitzdorf, 1984). The recordings in the same track were reproducible, as verified by recording during retraction of the electrode. This was done on four sample tracks and no substantial differences could be observed.

To further investigate the reproducibility of the cortical activation pattern under different anaesthesia, isoflurane in combination with N_2O was used in two CDCs. The pharmacological effect of ketamine and isoflurane is mainly on the excitatory synaptic transmission (Zuo *et al.*, 1996; Newcomer *et al.*, 1999). Isoflurane also acts on inhibitory synaptic transmission (Irifune *et al.*, 1997; Wakasugi *et al.*, 1999). Using the same criteria of anaesthesia depth (Kral *et al.*, 1999), the two anaesthetics used did not lead to significant differences in the field potentials and gross synaptic currents.

Synaptic Activity

Normal Hearing Acutely Deafened Cats (Controls)

The pattern of gross excitatory synaptic currents in normal hearing acutely deafened cats corresponds well to the data from acoustically stimulated squirrel monkey auditory cortex (Müller-Preuss and Mitzdorf, 1984) and cat visual cortex (Mitzdorf, 1985; Friauf and Shatz, 1991). Fishman *et al.* report very similar patterns of excitation (as revealed by CSD analysis) in the auditory cortex of the macaque monkey, although no depth or cortical layer verification was performed (Fishman *et al.*, 1998).

The present results from normal cats demonstrate the typical

temporal sequence of cortical layer activation in the primary auditory cortex. The shortest latency was demonstrated in gross synaptic currents in infragranular layers. Layers I, III, IV, V and VI are known to receive direct thalamocortical connections (Mitani *et al.*, 1985; Prieto *et al.*, 1994). Therefore, it is assumed that the short-latency gross synaptic currents in the infragranular layers reflect this direct thalamocortical input. Layer IV is the principal input layer of the cortex with most thalamocortical synapses (Niimi and Naito, 1974). This layer contains stellate cells, and it has been assumed that most synapses are formed with this cell type. Synapses to stellate cells would explain the smaller amplitudes of the sinks. Stellate cells have no preferential (vertical) orientation and a rather small size. Thus the spatial resolution of the CSD method (300 μm) may not suffice to consistently reveal all sinks and sources from these cells. Consequently, the infragranular sinks, which are more reproducible, may appear to show shorter latency over the ROI than sinks from layer IV. Additionally, our latencies are given as peak latencies. A closer inspection of Figure 4 [which fits data from e.g. (Müller-Preuss and Mitzdorf, 1984; Friauf and Shatz, 1991)] reveals similar onset latencies of the earliest sinks in layer IV and V/VI in the hearing cat, but a considerably shorter peak latency in layer V/VI.

Layer-specific latency studies are based on multi-unit recordings. These have a spatial resolution of tenths of micrometers, which is finer than the CSD method (steps of the order of hundreds of micrometers; in the present study 150–300 μm). The present study investigates synaptic currents which may also be subthreshold. Differences can therefore be expected, although some multi-unit studies also demonstrate their smallest latencies in layer VI (Sugimoto *et al.*, 1997).

A possible explanation of the temporal pattern of gross synaptic currents observed in normal cats (examples in Figs 3 and 4*a*) is presented in a model of cortical interconnections shown schematically in Figure 7*a*. It is based on latency differences between gross synaptic currents in different cortical layers. The assumption was that gross synaptic currents in one layer are caused by direct functional connections from layers which were activated <2 ms before. This model is compatible with the schemes published earlier according to anatomical and functional connections (Mitani *et al.*, 1985; Aitkin, 1990; Prieto *et al.*, 1994). According to the present results, a coactivation of layers III, IV, V and VI by thalamocortical afferents can be expected first (the CSD method does not allow layer I to be investigated). This is in agreement with Mitani *et al.* (Mitani *et al.*, 1985), who found coactivation of layers I, III, IV, V and VI. Prieto *et al.* (Prieto *et al.*, 1994) also describe thalamocortical connections in layers I, III, IV and VI. According to the CSD analysis, an excitation of cells in supragranular layers follows this input activity. The activity of supragranular layers is then relayed to the cells in the infragranular layers. Thereafter, there appears to be a rather complicated activation of both supra- and infragranular layers. This is assumed to be caused by intracortical circuits (both vertical and tangential). Tangential intracortical connections are very important in the processing of sensory stimuli and might be crucial for complex analyses (Winguth and Winer, 1986; Maunsell and Newsome, 1987; Singer, 1995; Katz and Shatz, 1996). An alternative explanation of the longer-latency currents might be that cortical neurons show intrinsic oscillatory responses (Gray and McCormick, 1996). The third possibility is an ongoing input from the thalamus in the time window investigated here (the first 50 ms post-stimulus). Nevertheless, there are several observations that indicate a simple onset activation of cortical networks from the thalamus in electrically stimulated normal cats. Single and multi-unit activity exhibits only a simple onset peak (sometimes bimodal) in the first 50 ms of the post-stimulus time histogram after electrical pulsatile stimulation in the cochlea [cat cortex (Raggio and Schreiner, 1994; Popelar *et al.*, 1995; Schreiner and Raggio, 1996; Hartmann *et al.*, 1997); inferior colliculus in cats and guinea pigs (Snyder *et al.*, 1995; Vischer *et al.*, 1997)]. The fourth possibility is that longer-latency currents represent rebound phenomena (Eggermont, 1992).

Congenitally Deaf Cats

In CDCs, CSDs show a different pattern of activation of the primary auditory cortex (Fig. 7*b*). Thalamic input is restricted to layers IV and V/VI. Layer IV gross synaptic currents show a loss in fine structure of the sinks in comparison with normal hearing cats. This might indicate functional deficits of the afferent auditory pathway (e.g. in thalamocortical afferents) as well as some changes in the layer IV neurons themselves.

The activity from layer IV is transferred to the supragranular layers. Activation of infragranular layers at longer latencies, which is believed to be caused by activity in supragranular layers (Fig. 7*a*) (Mitani *et al.*, 1985; Prieto *et al.*, 1994), is substantially reduced in CDCs. The infragranular layers are the output layers of the cortex. They provide input to other cortical areas and are the origin of efferent connections to the thalamus. Loss of activity in these layers indicates that the activity in the naive cortex is not propagated to the normal targets. Layers V and VI are the major sources of corticothalamic projection (Andersen *et al.*, 1980; Wong and Kelly, 1981; Mitani and Shimokouchi, 1985). Thalamo-cortico-thalamic loops (Steriade, 1997; de Venecia *et al.*, 1998) are therefore probably not functional in CDCs. The normal centrifugal projection to the inferior colliculus, which originates in layer V (Andersen *et al.*, 1980, Mitani *et al.*, 1983), is probably affected as well. Commissural fibres to the contralateral auditory cortex might be less affected by congenital deprivation, as these fibres originate not only in layer VI but also in layer III (Imig and Brugge, 1978; Wong and Kelly, 1981). The major source of output to AII are layers III and V in normal AI (Winguth and Winer, 1986). As some activity is preserved in layer III in CDCs, AII (if functionally present) might receive inputs.

The reasons for the insufficiencies observed in CDC primary auditory cortex are not known. Three possible hypotheses are:

1. The CDCs miss a critical period of development which is dependent on functional activation of the auditory system. Normal development of neural connections cannot therefore take place. In addition, it is known that the spontaneous activity in the auditory nerve in adult CDCs is substantially reduced (Ryugo *et al.*, 1998). Whether this important shaping influence in development is also reduced in neonatal CDCs is unknown.
2. The CDCs initially develop a normal auditory system. This, due to lack of activation, degenerates.
3. Both mechanisms mentioned above take place.

At present there is no published material available to support either of these hypotheses. Equipping the CDCs with a cochlear implant at an early age replaces auditory experience and indicates reversibility of the described changes (Klinke *et al.*, 1999). The study has demonstrated that chronic electrical stimulation with biologically relevant stimuli leads to:

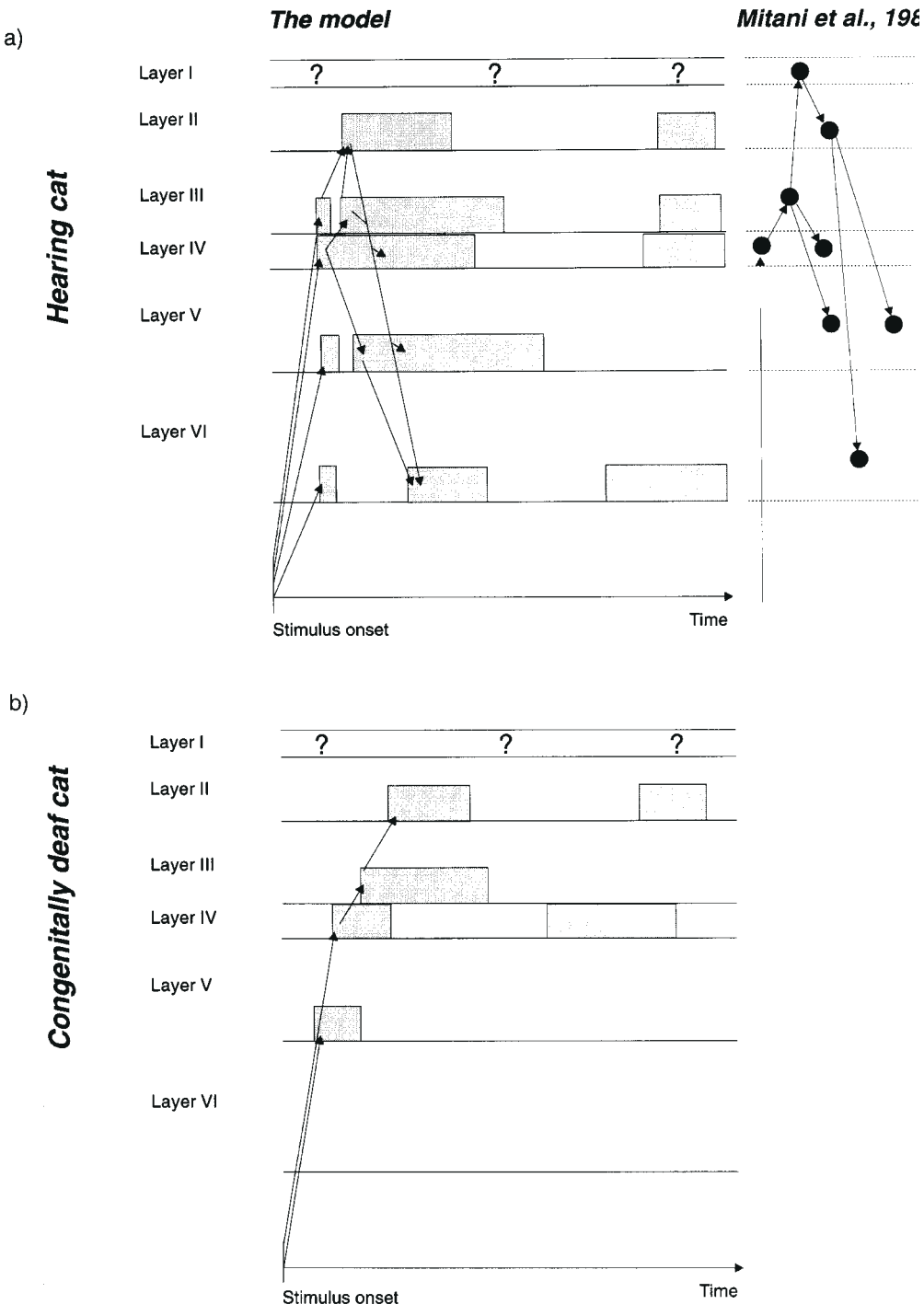

Figure 7. A model of auditory cortical activation based on the gross excitatory synaptic activity as revealed by the CSD method. (*a*) Activation of cells in cortical layers according to the presented data. The abscissa represents the post-stimulus time, the ordinate the cortical depth. Activation is shown as grey rectangles. Arrows show hypothetical connections based on the response latencies. Layer I activation is not shown, as the CSD method allows only limited conclusions about layer I. On the right, the model from Mitani *et al.* (Mitani *et al.*, 1985) according to morphological and functional investigations is shown. (*b*) The corresponding model of a congenitally deaf animal. Hypothetical connections are shown as arrows.

1. an increase in the amplitudes of the field potentials;
2. appearance of long-latency components (>150 ms) in the field potentials following chronic electrostimulation, absent in naive CDCs;
3. expansion of the cortical area devoted to the processing of auditory stimuli; and
4. normal activation of the cortical layers.

Whether there is a critical period outside of which such maturation cannot be achieved is under study. Apart from sink amplitudes, the present data demonstrate similar quantitative measures of synaptic currents in the youngest CDCs to hearing cats. In older CDCs there is a decreasing trend with age (Table 1). This finding may represent an indication of a 'sensitive period'.

The changes described in the present paper could also be

based on changes in the function of the afferent auditory pathway as well as changes in the auditory cortex. Dramatic effects of unilateral cochlear ablation have been demonstrated in the brainstem of Mongolian gerbils (Kitzes *et al.*, 1995). Changes in the afferent auditory pathway certainly will affect the input to the auditory cortex, and thus also influence the evoked cortical activity.

Several histological studies have been undertaken on CDCs. Larsen and Kirchhoff found that the end bulbs of Held in adult CDCs resemble immature synapses of young kittens (Larsen and Kirchhoff, 1992). They demonstrated a decrease in the cross-sectional area of the soma of large spherical cells in the CDCs, accompanied by a dramatic increase in both the pre- and postsynaptic membranes. CDCs have fewer and thinner branches of the end bulbs, which also have fewer varicosities and fewer terminal swellings (Ryugo *et al.*, 1997, 1998). There is a reduction of presynaptic vesicle density. Postsynaptic densities are thicker and expanded. Heid (Heid, 1998) showed a significant reduction in somatic areas of neurons in the cochlear nucleus, superior olivary complex and lateral lemniscus in adult CDCs [see also (Saada *et al.*, 1996)]. On the other hand, CDCs have preserved nucleotopic projections in the brainstem (Heid *et al.*, 1997). Similar results have also been presented for deafened ferrets (Moore, 1990). Hardie *et al.* demonstrated morphological changes in the inferior colliculus of neonatally bilaterally deafened cats (Hardie *et al.*, 1998). There was a significant reduction in number of synapses. No decrease of neuronal counts has been reported in the brainstem of auditory deprived cats. Cochlear ablation leads to such effects in, for example, birds (Born and Rubel, 1985).

In spite of these morphological data, only limited functional deficits could be demonstrated in the central auditory system of CDCs and neonatally deafened cats. In studies in the inferior colliculus of neonatally deafened cats, Snyder *et al.* (Snyder *et al.*, 1990, 1991, 1995) showed that

1. the cochleotopic organization of the inferior colliculus is basically unaffected by auditory deprivation;
2. basic response properties of units in the inferior colliculus are unaffected by neonatal deafening, as shown in peri-stimulus time histograms; and
3. the temporal resolution of units in the inferior colliculus of deprived cats is only slightly worse than in hearing cats.

Hartmann *et al.* (Hartmann *et al.*, 1996) reported similar results for the inferior colliculus of CDCs; furthermore, they recorded multi-units in the auditory cortex of CDCs (Hartmann *et al.*, 1997). Their post-stimulus time histograms do not exhibit substantial differences from electrically stimulated normal cats. A rudimentary cochleotopy has also been demonstrated (Hartmann *et al.*, 1997). Hardie and Shepherd demonstrated a significant increase in the threshold of electrically evoked brainstem responses in neonatally deafened animals (Hardie and Shepherd, 1999). A more pronounced increase in latency and threshold of wave IV has also been described. Nevertheless, these findings might relate to the loss of auditory nerve fibres and their demyelination, which is a consequence of application of ototoxic drugs (Hardie and Shepherd, 1999). On the other hand, a weakening of excitatory synapses as a consequence of congenital deprivation has been demonstrated in brain slices of gerbils after neonatal cochlear ablation (Kotak and Sanes, 1997).

Thus, with the exception of an increased stimulation threshold, the functional thalamocortical input to the auditory cortex of CDCs seems relatively unaffected. The effect of such a possible decreased excitability was balanced in this study by using a relative criterion for stimulation current. The stimulation intensity was related to the threshold of cortical field potentials in each cat (10 dB over individual threshold). The differences in response latencies, as observed in the brainstem, could have influenced the first latencies in the cortical sinks, but an unequal effect on latency in different layers, as shown in Figure 5, cannot be explained simply by increased latencies in the brainstem. The differences observed in this study are thus most probably of cortical origin. For the same reason, the dramatic decreases in amplitude of the sinks are most probably of cortical origin. Last but not least, the substantial differences in the temporal sequence of cortical layer activation between normal cats and CDCs cannot be explained by an overall decrease of responsiveness or change in cortical input. The same arguments can be applied to the reduction of synaptic currents with longer latencies and in infragranular layers.

A functionally deficient primary auditory cortex, as observed in the present study, should also show morphological differences to normal cortices. Indeed, morphological data from CDCs show a significant reduction in the number of primary dendrites in pyramidal cells (Wurth *et al.*, 1999). A reduction in the span of dendritic trees was also observed in the cortex. This would imply a reduction in the number of synapses, which in turn should diminish synaptic activity, as was shown in this study.

The question of what happens to the primary auditory cortex in congenital deafness remains. It has been suggested that it is recruited by the visual system in the CDC (Rebillard *et al.*, 1977, 1980). This finding could not be reproduced in our laboratory (Hartmann *et al.*, 1997). The present study on synaptic currents demonstrates functional impairments in the interlayer connections of the auditory cortex. This supports the hypothesis that the auditory cortex, at least the region which corresponds to AI in hearing cats, is deprived of input. Furthermore, the morphological data on the cortical neurons in CDCs with a significant reduction of the number of primary dendrites support this view. If the cortex was recruited by some other modality, there should be no pronounced deficits observable. Nevertheless, the possibility that the recruiting system might activate the auditory cortex in a manner different to the normal auditory input remains open. This could lead to functional impairments in response to auditory input and to morphological differences in some neuronal populations. Nevertheless, recent data on the visual system also support our view. In the naive visual system, no substantial recruitment of area 17 by the auditory system could be found (Yaka *et al.*, 1999).

Conclusions

The data presented above demonstrate functional deficits of the primary auditory cortex of CDCs (naive auditory cortex). When passing the first 6 months of life without auditory experience, the normal functioning of the auditory cortex is impaired. The naive auditory cortex does not generate significant activity in the infragranular layers. The activation of supragranular layers is temporally delayed and the amplitudes of synaptic currents are significantly smaller. Our results suggest that the observed changes are caused by degeneration or failing maturation of cortico-cortical and cortico-thalamic connections.

Notes

Dr Jean Smolders is thanked for his numerous critical comments. The authors would like to thank the COCHLEAR Co. for donation of the implants. The technical assistance of Ms Natalie Krimmel is acknowledged. Supported by the DFG (SFB 269).

Address correspondence to A. Kral, Physiologisches Institut III, Theodor-Stern-Kai 7, D-60590 Frankfurt am Main, Germany. Email: kral@em.uni-frankfurt.de.

References

Aitkin L (1990) The auditory cortex. London: Chapman & Hall.

Andersen RA, Knight PL, Merzenich MM (1980) The thalamocortical and corticothalamic connections of AI, AII and anterior auditory field (AAF) in the cat: evidence for largely segregated systems. J Comp Neurol 194:663–701.

Blakemore C (1978) Maturation and modification in the developing visual system. In: Handbook of sensory physiology, vol. III. Perception (Held R, Leibowitz HW, Teuber HL, eds), pp. 377–436. Berlin: Springer-Verlag.

Born DE, Rubel EW (1985) Afferent influences on brain stem auditory nuclei of the chicken: neuron number and size following cochlea removal. J Comp Neurol 231:435–445.

Brown KT, Tasaki K (1961) Localization of electrical activity in the cat retina by an electrode marking method. J Physiol (Lond) 158:281–295.

Buisseret P, Imbert M (1976) Visual cortical cells: their developmental properties in normal and dark-reared kittens. J Physiol 255:511–525.

Busby PA, Tong YC, Clark GM (1992) Psychophysical studies using multi-electrode cochlear implant in patients who were deafened early in life. Audiology 31:95–111.

Chugani HT, Müller RA, Chugani DC (1996) Functional brain reorganization in children. Brain Dev 18:347–356.

Cynader M, Berman N, Hein A (1976) Recovery of function in cat visual cortex following prolonged deprivation. Exp Brain Res 25:139–156.

de Venecia RK, Smelser CB, McMullen NT (1998) Parvaglobulin is expressed in a reciprocical circuit linking the medial geniculate body and auditory neocortex in the rabbit. J Comp Neurol 400:349–362.

Eddington DK, Dobelle WH, Brackmann DE, Mladejovsky MG, Parkin JL (1978) Auditory prostheses research with multiple channel intracochlear stimulation in man. Ann Otol Rhinol Laryngol Suppl 53:5–39.

Eggermont JJ (1992) Stimulus induced and spontaneous rhythmic firing of single units in cat primary auditory cortex. Hear Res 61:1–11.

Fishman YI, Reser DH, Arezzo JC, Steinschneider M (1998) Pitch v. spectral encoding of harmonic complex tones in primary auditory cortex of the awake monkey. Brain Res 786:18–30.

Friauf E, Shatz CJ (1991) Changing pattern of synaptic input to subplate and cortical plate during development of visual cortex. J Neurophysiol 66:2059–2071.

Fryauf-Bertschy H, Tyler RS, Kelsay DMR, Gantz BJ, Woodworth GG (1997) Cochlear implant use by prelingually deafened children: the influences of age at implant and length of device use. J Speech Lang Hear Res 40:183–199.

Gray CM, McCormick DA (1996) Chattering cells: superficial pyramidal neurons contributing to the generation of synchronous oscillations in the visual cortex. Science 274:109–113.

Hardie NA, Shepherd RK (1999) Sensorineural hearing loss during development: morphological and physiological response of the cochlea and auditory brainstem. Hear Res 128:147–165.

Hardie NA, Martsi-McClintock A, Aitkin L, Shepherd RK (1998) Neonatal sensorineural hearing loss affects synaptic density in the auditory midbrain. NeuroReport 9:2019–2022.

Harrison RV, Nagasawa A, Smith DW, Stanton S, Mount RJ (1991) Reorganization of auditory cortex after neonatal high frequency hearing loss. Hear Res 54:11–19.

Hartmann R, Topp G, Klinke R (1984) Discharge patterns of cat primary auditory fibers with electrical stimulation of the cochlea. Hear Res 13:47–62.

Hartmann R, Heid S, Klinke R (1996) Neuronal activity in the auditory cortex and inferior colliculus of congenitally deaf white cats evoked by electrical cochlear stimulation. In: Proceedings of the 24th Göttingen Neurobiology Conference (Elsner N, Schnitzler H-U, eds), vol. II, p. 460. Stuttgart: Thieme Verlag.

Hartmann R, Shepherd RK, Heid S, Klinke R (1997) Response of the primary auditory cortex to electrical stimulation of the auditory nerve in the congenitally deaf white cat. Hear Res 112:115–133.

Heid S (1998) Morphometrische Befunde am peripheren und zentralen auditorischen System der kongenital gehörlosen Katze. PhD Thesis, J.W. Goethe University, Frankfurt am Main.

Heid S, Jähn-Siebert TK, Klinke R, Hartmann R, Langner G (1997) Afferent projection pattern in the auditory brainstem in normal cats and congenitally deaf white cats. Hear Res 110:191–199.

Heid S, Hartmann R, Klinke R (1998) A model for prelingual deafness, the congenitally deaf white cat – population statistics and degenerative changes. Hear Res 115:101–112.

Hubel DH, Wiesel TN (1970) The period of susceptibility to the physiological effects of unilateral eye closure in kittens. J Physiol (Lond) 206:419–436.

Imbert M, Buisseret P (1975) Receptive field characteristics and plastic properties of visual cortical cells in kittens reared with or without visual experience. Exp Brain Res 22:25–36.

Imig TJ, Brugge JF (1978) Sources and terminations of callosal axons related to binaural and frequency maps in primary auditory cortex of the cat. J Comp Neurol 182:637–660.

Irifune M, Sato T, Nishikawa T, Masuyama T, Nomoto M, Fukuda T, Kawahara M (1997) Hyperlocomotion during recorvery from isoflurane anesthesia is associated with increased dopamine turnover in the nucleus accumbens and striatum in mice. Anesthesiology 86: 464–475.

Juliano SL (1998) Mapping the sensory mosaic. Science 279:1653–1654.

Katz LC, Shatz CJ (1996) Synaptic activity and the construction of cortical circuits. Science 274:1133–1138.

Kilgard MP, Merzenich MM (1998) Cortical map reorganization enabled by nucleus basalis activity. Science 279:1714–1718.

Kitzes LM, Kageyama GH, Semple MN, Kil J (1995) Development of ectopic projections from the ventral cochlear nucleus to the superior olivary complex induced by neonatal ablation of the contralateral cochlea. J Comp Neurol 353:341–363.

Klinke R, Kral A, Heid S, Tillein J, Hartmann R (1999) Recruitment of the auditory cortex in congenitally deaf cats by long-term electrostimulation through a cochlear implant. Science 285:1729–1733.

Kotak VC, Sanes DH (1997) Deafferentation weakens excitatory synapses in the developing central auditory system. Eur J Neurosci 9: 2340–2347.

Kral A, Hartmann R, Mortazavi D, Klinke R (1998) Spatial resolution of cochlear implants: the electrical field and excitation of auditory afferents. Hear Res 121:11–28.

Kral A, Tillein J, Hartmann R, Klinke R (1999) Monitoring of anaesthesia in neurophysiological experiments. NeuroReport 10:781–787.

Larsen SA, Kirchhoff TM (1992) Anatomical evidence of synaptic plasticity in the cochlear nuclei of white-deaf cats. Exp Neurol 115:151–157.

LaVail JH, LaVail MM (1972) Retrograde axonal transport in the central nervous system. Science 176:1416–1417.

Leake-Jones PA, Vivion MC, O'Reilly BF, Merzenich MM (1982) Deaf animal models for studies of a multichannel cochlear prosthesis. Hear Res 8:225–246.

Leventhal AG, Hirsch HB (1980) Receptive field properties of different classes of neurons in visual cortex of normal and dark-reared cats. J Neurophysiol 43:1111–1132.

Maunsell JHR, Newsome WT (1987) Visual processing in monkey extrastriate cortex. Annu Rev Neurosci 10:363–401.

McMullen NT, Goldberger B, Suter CM, Glaser EM (1988) Neonatal deafening alters nonpyramidal dendrite orientation in auditory cortex: a computer microscopic study. J Comp Neurol 267:92–106.

Merzenich MM, Knight PL, Roth GL (1975) Representation of cochlea within primary auditory cortex of the cat. J Neurophysiol 38: 231–249.

Mesulam MM (1976) The blue reaction product in horseradish peroxidase neurohistochemistry: incubation parameters and visibility. J Histochem Cytochem 24:1273–1280.

Mitani A, Shimokouchi M (1985) Neuronal connections in the primary auditory cortex: an electrophysiological study in the cat. J Comp Neurol 235:417–429.

Mitani A, Shimokouchi Mnomura S (1983) Effects of stimulation of the primary auditory cortex upon colliculogeniculate neurons in the inferior colliculus of the cat. Neurosci Lett 42:185–189.

Mitani A, Shimokouchi M, Itoh K, Nomura S, Kudo M, Mizuno N (1985) Morphology and laminar organization of electrophysiologically

identified neurons in the primary auditory cortex in the cat. J Comp Neurol 235:430–447.
Mitzdorf U (1985) Current source density method and application in cat cerebral cortex: investigations of evoked potentials and EEG phenomena. Physiol Rev 65:37–100.
Moore D (1990) Auditory brain stem of the ferret — bilateral cochlear lesions in infancy do not affect the number of neurons projecting from the cochlear nucleus to the inferior colliculus. Dev Brain Res 54: 125–130.
Moore JK, Niparko JK, Perazzo LM, Miller MR, Linthicum FH (1997) Effect of adult-onset deafness on the human central auditory system. Ann Otol Rhinol Laryngol 106:385–390.
Müller-Preuss P, Mitzdorf U (1984) Functional anatomy of the inferior colliculus and the auditory cortex: current source density analyses of click evoked potentials. Hear Res 16:133–142.
Neville HJ, Lawson D (1987) Attention and peripheral visual space in a movement detection task. III. Separate effects of auditory deprivation and acquisition of a visual language. Brain Res 405:284–294.
Newcomer JW, Farber NB, Jevtovic-Todorovic V, Selke G, Melson AK, Hershey T, Craft S, Olney JW (1999) Ketamine-induced NMDA receptor hypofunction as a model of memeory impairment and püsychosis. Neuropsychopharmacology 20:106–118.
Nicholson C, Freeman JA (1975) Theory of current source density analysis and determination of conductivity tensor for an auran cerebellum. J Neurophysiol 38:356–368.
Niimi K, Naito F (1974) Cortical projections of the medial geniculate body of the cat. Exp Brain Res 19:326–342.
Niparko JK, Finger PA (1997) Cochlear nucleus cell size changes in the dalmatian: model of congenital deafness. Otolaryngol Head Neck Surg 117:229–235.
Nishimura H, Hashikawa K, Doi K, Iwaki T, Watanabe Y, Kusuoka H, Nishimura T, Kubo T (1999) Sign language 'heard' in the auditory cortex. Nature 397:116.
Phillips DP, Irvine DRF (1981) Responses of single neurons in physiologically defined primary auditory cortex (AI) of the cat: frequency tuning and responses to intensity. J Neurophysiol 45: 48–58.
Ponton CW, Don M, Eggermont JJ, Waring MD, Kwong B, Masuda A (1996) Auditory system plasticity after long periods of complete deafness. NeuroReport 8:61–65.
Popelar J, Hartmann R, Syka J, Klinke R (1995) Middle latency responses to acoustical and electrical stimulation of the cochlea in the cats. Hear Res 92:63–77.
Prieto JJ, Peterson BA, Winer JA (1994) Morphology and spatial distribution of GABAergic neurons in cat primary auditory cortex. J Comp Neurol 344:349–382.
Raggio MW, Schreiner CE (1994) Neural responses cat primary auditory cortex to electrical stimulation. I. Intensity dependence of firing rate and response latency. J Neurophysiol 72:2334–2359.
Rauschecker J (1991) Mechanisms of visual plasticity: Hebb synapses, NMDA receptors and beyond. Physiol Rev 71:587–615.
Reale RA, Imig TJ (1980) Tonotopic organisation in auditory cortex of the cat. J Comp Neurol 192:265–291.
Rebillard G, Carlier E, Rebillard M, Pujol R (1977) Enhancement of visual responses on the primary auditory cortex of the cat after an early destruction of cochlear receptors. Brain Res 129:162–164.
Rebillard G, Rebillard M, Pujol R (1980) Factors affecting the recording of visual-evoked potentials from the deaf cat primary auditory cortex (A1). Brain Res 188:252–254.
Reid SNM, Daw NW (1995) Dark-rearing changes dendritic microtubule-associated protein 2 (MAP2) but not subplate neurons in cat visual cortex. J Comp Neurol 359:38–47.
Reinoso-Suarez F (1961) Topographischer Hirnatlas der Katze. Darmstadt: E. Merck AG.
Robertson RT (1987) A morphometric role for transiently expressed acetylcholine esterase activity in the developing thalamocortical systems? Neurosci Lett 75:259–264.
Robertson RT, Motamond F, Kageyama GH, Gallardo KA (1991) Primary auditory cortex in the rat: transient expression of acetylcholine esterase activity in developing geniculocortical projection. Devl Brain Res 58:81–95.
Ryugo DK, Pongstaporn T, Huchton DM, Niparko JK (1997) Ultrastructural analysis of primary endings in deaf white cats: morphologic alterations in end bulbs of Held. J Comp Neurol 385:230–244.
Ryugo DK, Rosenbaum BT, Kim PJ, Niparko JK, Saada AA (1998) Single unit recordings in the auditory nerve of the congenitally deaf white cats: morphological correlates in the cochlea and the cochlear nucleus. J Comp Neurol 397:532–548.
Saada AA, Niparko JK, Ryugo DK (1996) Morphological changes in the cochlear nucleus of congenitally deaf white cats. Brain Res 736:315–328.
Sachs L (1968) Statistische Auswertungsmethoden. Berlin: Springer-Verlag.
Schreiner CE, Raggio MW (1996) Neural responses in cat primary auditory cortex to electrical stimulation. II. Repetition rate coding. J Neurophysiol 75:1283–1300.
Singer W (1995) Development and plasticity of cortical processing architectures. Science 270:758–764.
Skuse DH (1993) Extreme deprivation in early childhood. In: Language development in exceptional circumstances (Bishop D, Mogford K, eds), pp. 29–46. Hove: Lawrence Erlbaum.
Snyder RL, Rebscher SJ, Cao K, Leake PA, Kelly K (1990) Chronic intracochlear electrical stimulation in the neonatally deafened cat. I. Expansion of central representation. Hear Res 50:7–34.
Snyder RL, Rebscher SJ, Leake PA., Kelly K, Cao K (1991) Chronic intracochlear electrical stimulation in the neonatally deafened cat. II. Temporal properties of neurons in the inferior colliculus. Hear Res 56:246–264.
Snyder R, Leake P, Rebscher S, Beitel R (1995) Temporal resolution of neurons in cat inferior colliculus to intracochlear electrical stimulation: effects of neonatal deafening and chronic stimulation. J Neurophysiol 73:449–467.
Steriade M (1997) Synchronized activities of coupled oscillators in the cerebral cortex and thalamus at different levels of vigilance. Cereb Cortex 7:583–604.
Stryker MP, Harris WA (1986) Binocular impuls blockade prevents the formation of ocular dominance columns in cat visual cortex. J Neurosci 6:2117–2133.
Sugimoto S, Sakurada M, Horikawa J, Taniguchi I (1997) The columnar and layer-specific response properties of neurons in the primary auditory cortex of Mongolian gerbils. Hear Res 112:175–185.
Suzuki H, Azuma M (1976) A glass-insulated 'Elgiloy' microelectrode for recording unit activity in chronic monkey experiments. Electroenceph Clin Neurophysiol 41:93–95.
Swindale NV (1988) Role of visual experience in promoting segregation of eye dominance patches in visual cortex of the cat. J Comp Neurol 267:472–488.
Vischer MW, Bajo WM, Zhang JS, Calciati E, Haenggeli CA, Rouiller EM (1997) Single unit activity in the inferior colliculus of the rat elicited by electrical stimulation of the cochlea. Audiology 36:202–227.
Wakasugi M, Hirota K, Roth SH, Ito Y (1999) The effects of general anaesthetics on excitatory and inhibitory synaptic transmission in area CA1 of the rat hippocampus *in vitro*. Anesthesiol Analg 88: 676–680.
Wakita M, Watanabe S (1997) Compensatory plasticity following neonatal lesion of the auditory cortex. Biomed Res 18(suppl. 1):79–89.
Weinberger N (1998) Tuning the brain by learning and by stimulation of the nucleus basalis. Trends Cogn Sci 2:271–273.
Winguth SD, Winer JA (1986) Corticocortical connections of cat primary auditory cortex (AI): laminar organization and identification of supragranular neurons projecting to area AII. J Comp Neurol 248:36–56.
Wong D, Kelly JP (1981) Differentially projecting cells in individual layers of the auditory cortex: a double labeling study. Brain Res 230:362–366.
Wurth NN, Heid S, Kral A, Klinke R (1999) Morphology of neurons in the primary auditory cortex (AI) in normal and congenitally deaf cats — a study of DiI labelled cells. Göttingen Neurobiol Rep 318.
Xu SA, Shepherd RK, Chen Y, Clark GM (1993) Profound hearing loss in the cat following the single co-administration of kanamycin and ethacrynic acid. Hear Res 70:205–215.
Yaka R, Yinon U, Wollberg Z (1999) Auditory activation of cortical visual areas in cats after early visual deprivation. Eur J Neurosci 11: 1301–1312.
Zuo Z, De Vente J, Johns RA (1996) Halothane and isoflurane dose-dependent inhibit the cyclic GMP increase caused by *N*-methyl-D-aspartate in rat cerebellum: novel lacalization and quantitation by *in vitro* autoradiography. Neuroscience 74:1069–1075.

Appendix

One-dimensional current source densities were computed off-line from the recorded field potentials (Mitzdorf, 1985). The one-dimensional CSD represents the second spatial derivative of the field potentials in the track direction. It is a scalar quantity which defines the amplitude of the source and sink of current at a given point [for theoretical details see e.g. (Nicholson and Freeman, 1975)]. Extracellular field potenitals result from the volume average of many small membrane currents. The CSD signal corresponds to the gross synaptic currents (essentially excitatory post-synaptic currents) of the cortical elements directed parallel to the electrode track (Mitzdorf, 1985). To a large extent it thus reflects the signals originating from pyramidal cells. By convention, the method assumes a constant resistivity, which is ignored. The amplitudes of the CSD signal are therefore given in mV/mm^2 (Mitzdorf, 1985). The sinks in the CSD are assumed to reflect post-synaptic inward currents which flow during synchronous activation of groups of excitatory synapses. The sources are supposed to correspond to passive, concomitant, outward currents (Müller-Preuss and Mitzdorf, 1984). The sinks of the CSD signals render a quantity relating to *gross synaptic currents*. ϕ_t^d represents the potentials recorded at cortical depth d at time t (Fig. 1*b*). Δd represents the distance between the recordings of field potentials in the cortex (150–300 μm; see above). The CSD can then be computed according to equation (1).

$$CSD_t^d = \frac{\phi_t^{d-\Delta d} - 2\phi_t^d + \phi_t^{d+\Delta d}}{(\Delta d)^2} \quad (1)$$

Track Reconstruction

The accuracy of the assignment of cortical layers to penetration depths was ensured by histological track reconstruction. The deviation angle (Fig. 3) in the histologically reconstructed tracks was 0–14°. The maximal possible deviation angle with the given adjustment of the stereotactical microelectrode holder was 36° according to the cat stereotactical brain atlas.

The accuracy of cortical layer assignment for given penetration depths is given by the span between the penetration depth (0° deviation) and cortical depths for the maximum possible deviation angle of 36°.

The assignment of layer IV was found to be accurate in the recorded area (Fig. 1*a*). Layer IV was found to extend from a cortical depth between 730 (minimum from nine positions in AI) and 1040 μm (maximum from nine positions in AI) in the histological preparations of both hearing and deaf cats. After correction for 11% tissue shrinkage, this corresponds to cortical depths of 810–1154 μm, which in turn corresponds to penetration depths of 900–1200 μm. Furthermore, all iron deposits at track depth 1000 μm were found in layer IV. The positions of layers II and III had to be extrapolated. As the track angle does not result in large differences in cortical depth for these small penetration depths, their assignment can be considered to be accurate. The depth error increases with increasing penetration depth. The assignment of deeper layers (infragranular layers V and VI) therefore becomes difficult for the unreconstructed tracks. The border of layers V and VI also depends on the distance from the sulci. To minimize errors in layer assignment, the differentiation to layers V and VI was not performed, and signals from these layers are given as layer V/VI in the text.